Estimation of Crops Water Consumptions Using Remote Sensing with Case Studies from Egypt

Mohammed A. El-Shirbeny, E. S. Mohamed, and Abdelazim Negm

Abstract Actual evapotranspiration (ETa) represents crop water consumption in consideration, the water conserved in plant tissue structure representing about 1% or less. Many researchers understood the importance of ETa, and they did their best to measure or calculate ETa. Tens of experimental and mathematical models were used to calculate evapotranspiration in last century. Many weather, plant, and soil parameters were inserted in these models. Most of these models were acceptable for local scale and used for certain climate. Only a very few models were used on a global scale but need a lot of parameters and well-distributed weather stations. The crop pattern was the main obstacle to using these models on a large scale. The early satellite age was the beginning of the development of global-scale models through using satellite images to calculate ETa and manage crop water consumption. Triangle and crop water stress index (CWSI) methods were used and developed in the 1970s and the 1980s, respectively. In 1990s and beginning of 2000s, the SEBAL and SEBS models represent a new step in the way of evapotranspiration development models. In the last decade, METRIC, ETLook, Alexi, and ET watch models were developed to fill the gaps of SEBAL and SEBS models. Researchers around the world still try to modify these models to improve the results.

Keywords Crop, Evapotranspiration, Modeling, Remote sensing, Water, Water consumption

---

M. A. El-Shirbeny (✉) and E. S. Mohamed
National Authority for Remote Sensing and Space Sciences (NARSS), Cairo, Egypt
e-mail: mshirbeny@yahoo.com; m.elshirbeny@narss.sci.eg

A. Negm
Water and Water Structures Engineering Department, Faculty of Engineering,
Zagazig University, Zagazig, Egypt

A. M. Negm (ed.), *Conventional Water Resources and Agriculture in Egypt*,
Hdb Env Chem, DOI 10.1007/698_2018_305,

Contents

1 Introduction

In the western USA, since about the 1890s, rationalization of water losses became more important. Water applied significantly exceeded the consumptive-use values [1]. After that date, many researchers started to formulate the water losses in the agriculture field. They tried to represent the physical processes of water losses from soil and plant leaves which is called ETa. The ETa can be measured correctly using weighing lysimeters and could be estimated from empirical methods. Unfortunately, these methods produce point values of ETa. It is used for a specific location and fails to provide the ETa on a regional scale, although it is costly. The ETa is calculated in many ways and steps.

ETa is the real amount of crop water consumption during all phonological stages from cultivation to senescence. It is affected with weather parameters, crop characteristics, and water availability [2]. To calculate ETa, many parameters must be inserted in the next equation:

$$\mathrm{ETa} = \mathrm{ETc} \times \mathrm{Ks} \tag{1}$$

$$\mathrm{ETc} = \mathrm{ETo} \times \mathrm{Kc} \tag{2}$$

where ETc is crop evapotranspiration (mm/day), ETo is reference evapotranspiration (mm/day), Kc is crop coefficient, and Ks is water stress coefficient.

The major limiting factors controlling ETo are water availability, amount of energy, and wind speed. These factors depend on many other quantities such as soil moisture, land surface temperature, air temperature, vegetation cover, vapor pressure, wind speed, which vary according to the latitude of the region, the season of the year, time of day, and cloud cover. It requires daily data to provide an acceptable estimation of crop water requirements [3].

Numerous models which varied in complexity were used to calculate ETo. Penman-Monteith method is one of the most accurate models to estimate ETo.

Recently, the modified FAO Penman-Monteith equation presented in the FAO paper 56 has been widely used to estimate both the hourly and daily ETo from climatic data, either measured in the field or official meteorological records [2].

The advancements in satellite, airborne, and ground-based remotely sensed data are extremely being used in agriculture. The use this data was evaluated in many agriculture activities. Many studies investigated the potentiality of remote sensing data in crop monitoring, yield prediction, weed control and pest management, and crop water requirements [4–10].

Oki and Kanae [11] predicted soil water availability for irrigation water management by the use of remotely sensed data. Remote sensing estimation of ET can help detect, map, and provide guidance for crop water requirements in irrigated lands [12]. It is also very beneficial in monitoring water stress in precision agriculture [13].

Remote sensing technique is a powerful, economic, and efficient tool for estimating ETa. The irrigated farms and crop coefficient (Kc) curves may be monitored and developed through remote sensing techniques [14]. Choudhury [15] proposed a method to assess solar radiation, air temperature, and vapor pressure deficit using remotely sensed data. The general approach to estimate physical parameters is using a combination of remote sensing data, ancillary data, and atmospheric data for ET estimation [16, 17]. Accurate characterization of global ET distribution with satellite remote sensing independent of ground observations is a very difficult task. The estimation of ET rates to both Ts and NDVI values derived from remotely sensed data using multiple regression analyses [18].

Ray and Dadhwal [19] used remote sensing and geographic information system tools for estimating seasonal ETc. They generated a ETc map from meteorological observations. They used meteorological data to compute ETo by using FAO Blaney-Criddle method.

The point data of ETo were interpolated using the inverse square distance approach available in ARC/INFO. However, they combined the Kc and ETo maps to generate seasonal ETc map. This technique can cover hundreds of fields.

Dibella et al. [18] tested the predictive power of models based on NDVI and surface temperature to estimate ET. They found a significant relationship with high correlation between temperature and NDVI data and ET.

$$\mathrm{ET} = a1(\mathrm{LST}) + a2(\mathrm{NDVI}) + b \tag{3}$$

where LST is land surface temperature, NDVI is normalized difference vegetation index, and $a1$, $a2$, and b are empirically coefficients.

Several studies have analyzed the relationship between ET flux and NDVI and surface temperature information generated from sensors onboard meteorological satellites [20]. Kalma et al. [21] reviewed most of evapotranspiration estimation by using remote sensing technique as follows.

2 The Water Stress Method

In the previous decade, many researchers studied and evaluated the crop water stress index (CWSI) for scheduling irrigation purposes [22–25]. The CWSI is detecting water stress (WS) remotely through the measurements of a crop's surface temperature (ST). The relation between ST and WS is based on cooling the plant leaves through transpiration. Under water shortage conditions, the crop's temperature will increase due to the increase in plant transpiration.

The prevalent used CWSI method [26, 27] depends theoretically on the observed canopy and air temperature differences as:

$$\mathrm{CWSI} = \left[(T_c - T_a) - (T_c - T_a)_{\min}\right] / \left[(T_c - T_a)_{\max} - (T_c - T_a)_{\min}\right] \quad (4)$$

where the subscripts min refers to unstressed conditions and conditions of maximum stress. The CWSI value ranged from 0 to 1. Zero is no water stress, and 1 represents fully water stress. The CWSI take into account the evaporation from the soil and crop. It could be interpreted as a measure of the amount of ET actually occurring relative to the ETc (Eq. 5).

$$\mathrm{CWSI} = 1 - \mathrm{ETa}/\mathrm{ETc} \quad (5)$$

Moran et al. [16] promoted the water deficit index (WDI) (see Fig. 1). The WDI is a function of ETa to ETc ratio [28]. Yield water stress response depends on crop type

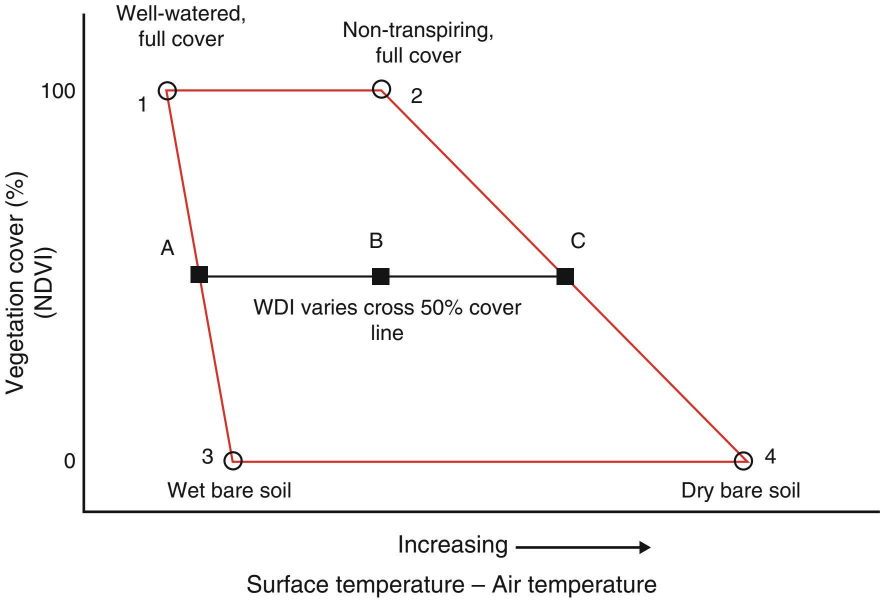

Fig. 1 Represents the WDI trapezoid

and the phonological stage, soil, and climatic conditions. The use of WDI in yield predictions or irrigation management requires estimation of WDI for that particular crop under different soil, growth stage, and climatic conditions [29]. Several satellite data sources were used to calculate WDI such as Landsat, NOAA/AVHRR, and MODIS. El-Shirbeny et al. [4] used NOAA/AVHRR to calculate WDI in the eastern part of Nile Delta, Egypt. A MODIS index based on the spatial relationship between LST and NDVI was evaluated by Garcia et al. [30] to estimate WDI in two sites with different climatic controls on ETa in Andalusia, Spain. It is found that accounting for the spatial variation in Tair is one of the most critical factors to achieve accurate estimation of the temperature vegetation dryness index (TVDI).

The crop started to detect water stress when the WDI is located to the right of the line connecting points 1 and 4 [31].

Although the calculated data is largely common, but it still needs calibration and validation with measuring data.

2.1 Case Study for Water Stress Method

El-Shirbeny et al. [32] applied the WDI on Elsalhyia region in the eastern part of Nile Delta. The results of ETa varied from 0 to 3.7 mm/day. ETa was affected by the changing in CWSI and ETc according to Eq. (5). As shown in Fig. 2, the variation of ETa was observed according to land cover type, crop stage, weather conditions, and water stress conditions.

In arid and semiarid climatic region, ET ranges over a large interval depending on water regimes. Moreover, the variation in one weather parameter immediately affects all the other which are mutually related. This fact makes it difficult to correctly evaluate the ETa [33]. Er-Raki et al. [34] have analyzed the efficiency of three methods based on the FAO-56 Kc approach to estimate ETa for winter wheat under different irrigation treatments in the semiarid conditions of Morocco. ETa (mm/day) is the product of an uptake coefficient (α, mm/day) and available water ($\theta - \theta$WP) when ETa is less than ETc (mm/day): If ETa $<$ ETc, ETa $= \alpha$ ($\theta - \theta$WP), and if ETa $\geq$ ETc, ETa $=$ ETc. ETc occurs when the availability of soil water does not limit transpiration [35], and it could be estimated using the FPM model [2].

3 Surface Energy Balance (SEB) Model

In the period from 1950s to 1960s, there was a belief that evapotranspiration from well-watered land surfaces was mainly controlled through weather data only. However, the variation of vegetation and soil parameters was an obstacle. By the 1980s, the scientists started to care about land surface parameters [21].

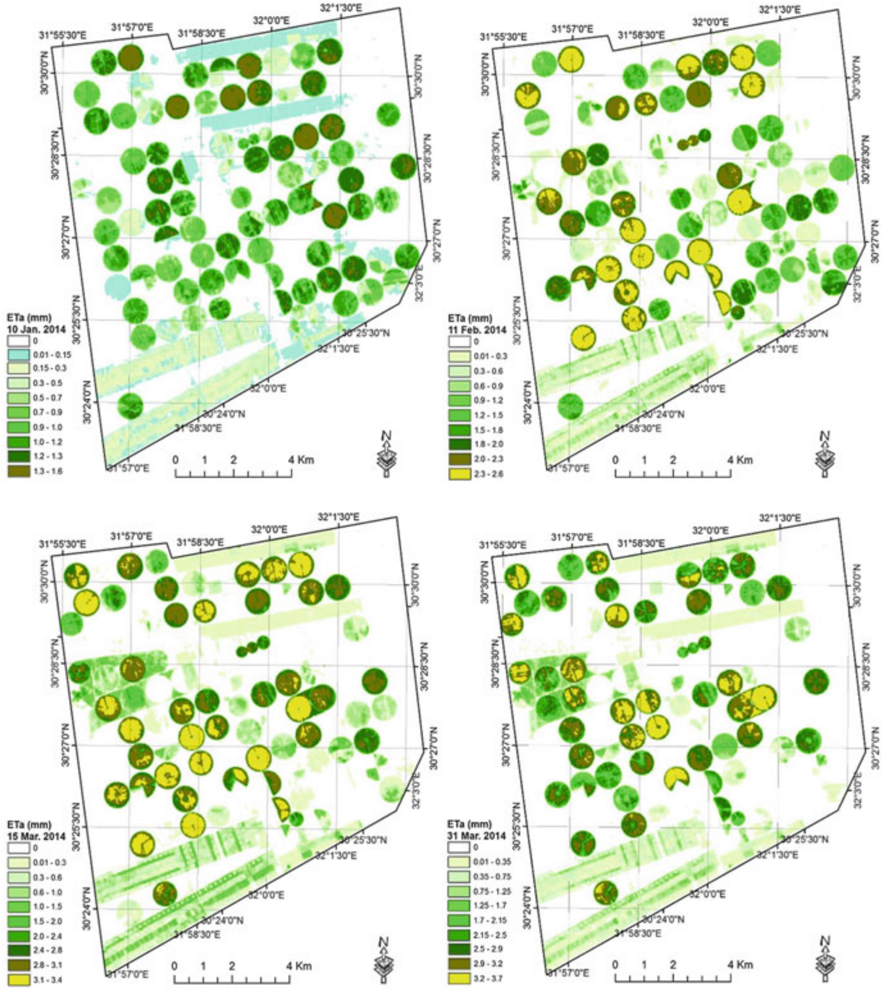

Fig. 2 Shows ETa distribution in the study area

SEB models were divided into two main groups. The first is one-source models, and the second is two-source models. The one-source models do not differentiate between evaporation from the soil and transpiration from the vegetation. Conversely, the two-source models distinguish between fluxes from the soil and the vegetation. The two-source models have been developed for use with incomplete canopies [36] (Fig. 3).

The SEB equation described as:

$$\mathrm{Rn} = \lambda \mathrm{E} + H + G \tag{6}$$

where G is soil heat flux, λE is latent heat flux, Rn is net radiant energy, and H is sensible heat flux. All units are expressed in W m^{-2}.

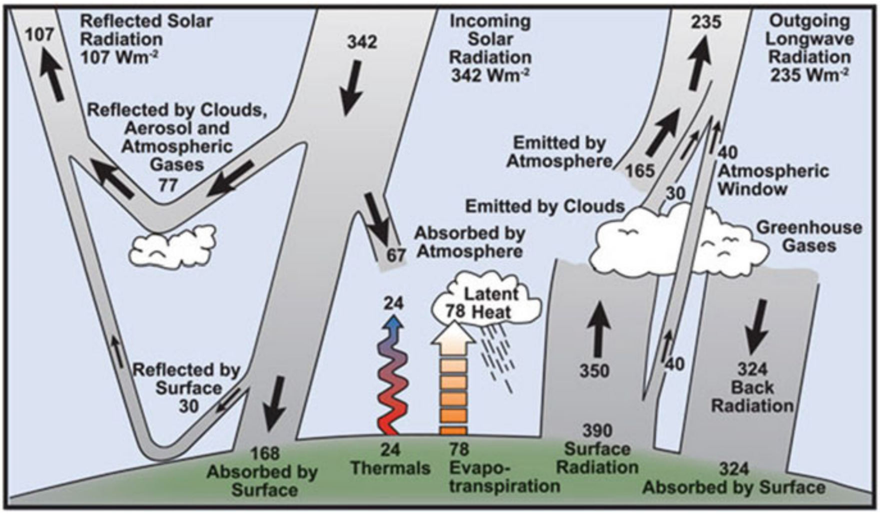

Fig. 3 Explains the physical theoretical concept of energy balance. Source: Kiehl and Trenberth [37]

E is the rate of water evaporation (kg m^{-2} s^{-1}), and λ is the latent heat of water vaporization (J kg^{-1}). All parameters of Eq. (6) are depending on the LST. The Rn term is taken as positive if it is a gain to the surface, whereas the other fluxes are taken as positive if they are away from the surface. Eq. (6) can be prepared as:

$$\mathrm{Rn} - G = \lambda\mathrm{E} + H \tag{7}$$

The part of (Rn $-$ G) is named the available energy. It is required for each SEB scheme. The radiation budget represented by Rn is written as:

$$\mathrm{Rn} = K\downarrow - K\uparrow + L\downarrow - L\uparrow \tag{8}$$

where $K\downarrow$ is downwelling shortwave radiation which depends on atmospheric transmissivity, time of day, day of year, and geographic position, $K\uparrow$ is reflected shortwave radiation which relies on surface albedo (α) and $K\downarrow$, $L\downarrow$ are downwelling longwave radiation (which relies on the atmospheric emissivity which in turn is affected by amounts of atmospheric water vapor, carbon dioxide, and oxygen and by air temperature), and $L\uparrow$ is upwelling longwave radiation (which relies on LST and emissivity). G, which normally ranged from 5 to 20% of Rn during daylight hours, relies on the soil's thermal conductivity and the vertical temperature gradient. LST impacts on all four terms of the energy balance of Eq. (1) and in particular on $L\uparrow$ in the radiation balance of Eq. (8) [21].

SEB models are determined through a solution of the surface energy budget. According to Su [38], three broad SEB approaches were used for determining a real ET. The first one estimates the sensible heat flux (H) and then gets the latent heat flux (λE) as the remaining of the energy balance equation. This so-called residual method is represented by:

$$\lambda E = Rn - G - H \tag{9}$$

All terms of this equation is described above. The second approach uses a water stress index to estimate the relative evaporation (Er), i.e., the ratio of real to potential evaporation (Ea/Ep).

As some of the SEB models are more complicated, need a large number of surface information, and depend on (Trad = LST) which specific sensors are provided, some attempts have been developed to estimate evapotranspiration. These attempts aimed to extract and estimate number of vegetation indices which are related to and describe the crop status and characteristics such as chlorophyll content, leaf area index, crop height, and vegetation to soil ratio. Using these indices helps to enter into the estimation of Kc that can be used beside ETo to estimate crop ET.

3.1 SEBAL Model

The Surface Energy Balance Algorithms for Land (SEBAL) methodology [39, 40] is applied with surface temperature, surface reflectivity, and NDVI data. The plan describes a one-source cover transfer plan which determines rs, H, λE, and near-surface soil moisture. The plan makes precise use of the detected spatial variability in surface temperature and surface reflectance over a single cloud-free view. SEBAL has been produced at the territorial scale, and it needs some collective ground-level measurements from within the view. $K\downarrow$ and $L\downarrow$ are calculated using a fixed atmospheric transmissivity, a suitable atmospheric emissivity value, and an experimental function of Ta, sequentially. G is determined as a portion of Rn depending on Trad, NDVI, and α [41].

SEBAL estimates the instant value of the sensible heat flux in three principal levels. It firstly recognizes that Taero is not equal to Trad. It concludes that the relationship between Trad and the gradient of surface temperature (ΔT) is represented as Taero. Two extremes are distinguished from the scene: a wet extreme where $\lambda E > H$ and $\Delta T = 0$ and a dry extreme where $\lambda E = 0$ and $H = Rn - G$. Secondly, a scatter plot is achieved for all pixels in the whole scene of broadband α values against Trad. Pixels with high ET rates ($\lambda E > H$) are assumed to have low temperature and low reflectance values, while regions with limited or no ET ($\lambda E \approx 0$ and $H \approx Rn - G$) possess high surface temperatures and commonly high reflectance values. Finally, H can be determined for each pixel with λE as the remaining term in Eq. (4) by using the local surface roughness (zom) based on the NDVI and the assumption of a fixed zom/zoh ratio. The SEBAL plan has been accepted internationally with space-borne and airborne data over approximately horizontal landscapes with and without irrigation [39, 40].

3.2 SEBS Model

The one-dimensional Surface Energy Balance System (SEBS) of Su [38] assesses heat fluxes through space-borne data and available weather data. SEBS needs three groups of input data. The first set consists of α, ε, Trad, LAI, partial vegetation coverage, and the plant height. If vegetation information is not accessible, the NDVI is used as a substitution. The second group involves measurements of Ta, u, real vapor pressure (ea) at a standard height, as well as complete air pressure. The third group of data involves observed (or determined) $K\downarrow$ and $L\downarrow$. SEBS is made up of various separate modules to determine Rn and G and divide the (Rn − G) into H and λE. H is answered using the similarity theory. SEBS has been assessed over farming, grassland, and forested sites and over different spatial scales. It has been used with tower-based data and with Landsat, ASTER, and MODIS space-borne data.

3.3 METRIC Model

The Mapping ET at high Resolution and Internalized Calibration (METRIC) method [42] was obtained from SEBAL. METRIC uses the crop's ETo to describe fully transpiring plants. Extreme (cool/wet and warm/dry) pixels are classified in the given agricultural perspective with the cool/wet extreme relative to a reference crop with its transpiration rate calculated from the Penman-Monteith incorporation equation. Evaporation from the warm/dry pixel is determined with a soil water budget utilizing local weather data. Field studies with irrigated alfalfa in Idaho gave approval to within 5% between METRIC estimations and lysimeter measurements. METRIC also uses the ETo to extrapolate from instantaneous ET fluxes to daily rates.

3.4 ETWatch Model

Wu et al. [43] produced ETWatch model which depended firstly on SEBAL model to calculate ETa. Wu et al. [44] developed the model to be a stand-alone model away from SEBAL. ETWatch is still a local Chinese model, but it started to go through the border outside China. The ETWatch model was applied for the first time outside China last year on Egypt.

3.5 ETLook

Numerous algorithms based on actual evapotranspiration (ET act) mapping using visible, near-infrared, and thermal data exist. The ET mapping of river basins and continents at a moderate resolution (1 km) is vital to detect the spatial heterogeneity of ET and its response to weather events (rainfall or drought). Surface energy balance techniques like RSEB [21], SEBI [45], SEBAL [39, 40], SEBS [38], and METRIC [42] estimate ET act as a latent heat flux (residual term in surface energy balance). The major challenge (or disadvantage) of these techniques is the need for thermal infrared data to assess surface temperature. Thermal infrared data cannot provide reliable estimates of surface temperature under cloudy or hazy conditions, rendering the algorithms less useful in temperate climates. The visible and near-infrared data are used to provide information on vegetation conditions and surface albedo for absorbed solar energy. These parameters are less critical to cloudy conditions, as their variation is not as significant and irregular as the surface temperature.

Verhoef [46] showed that missing data of NDVI and surface albedo could be estimated using observations from other data. ETLook is specially developed to map ET act for large areas on a daily to weekly basis for more extended time periods with a resolution of 1 km. Typical outputs consist of yearly ET act with an interval of 1 week associated with biomass growth and with an interval of 2 weeks for large watersheds. Sufficient detail within the watersheds can be used to monitor local differences in water management.

ETLook is a newly developed algorithm to compute ET act of large areas using soil moisture estimates from the passive microwave sensor AMSRE. A drawback of the passive microwave sensor data is the low resolution of the data. The global soil map was used to downscale the soil moisture from the AMSRE sensor.

ETLook uses moderate resolution VNIR images from the MODIS sensor for defining surface albedo and vegetation cover. Regular weather measurements (wind speed, air temperature, and relative humidity) at a number of stations inside the study area are used to conclude the current meteorological conditions. Because the main driving power of the process is soil moisture derived from passive microwave sensors, the algorithm is appropriate under all weather conditions. Therefore the algorithm can be used operationally, making it useful for real-time hydrological modeling and operational land surface models.

3.6 A Case Study for SEB Method

A case study on Nile Delta, using METEOSAT measurements, was studied by Bastiaanssen et al. [39, 40].

The water balance models usually compute ET from vegetation and bare soil based on the unstressed transpiration and bare soil potential evaporation. Empirical reduction factors related to actual soil moisture content and salinity are then applied to correct for less optimal soil water and salinity conditions. When this category of models is locally calibrated against soil water, groundwater table variation, and return flow, they give reasonable estimates of regional evaporation [39, 40].

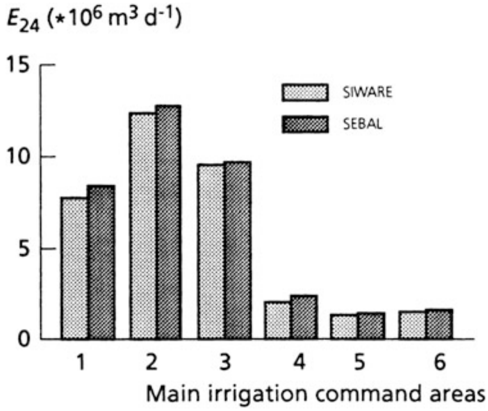

Fig. 4 Relative difference in daily evaporation between SIWARE and SEBAL for the six main irrigation command areas. The numbers represent the (1) Ismaileya, (2) Rayah Tawfiki, (3) Mansureya, (4) Sharqaweya, (5) Bassoseya, and (6) Abu Managa areas [39, 40]

Pelgrum [47] studied the water consumption of the irrigated Nile Delta. An attempt was made to determine the surface energy balance for each daytime hour using METEOSAT. The 24-h SEBAL evaporation rates obtained for the Nile Delta were compared by Bastiaanssen et al. [17] with the 24-h evaporation figures obtained from the calibrated hydrological model SIWARE [48]. At the time of image acquisition in August 1986, maize, cotton, orchards, and vegetables were grown on the irrigated Nile Delta. The SIWARE network in the Eastern Nile Delta governorates is 82 irrigation units. The total gross irrigated area covered by the 82 irrigation units is 695,000 ha. The results for six irrigation commands are demonstrated in Fig. 4. The relative error of the command areas DE24/E24 (SIWARE-SEBAL)/SIWARE appeared to be small (see Fig. 4), with a mean for the six cases of DE24/E24 = −0.08 and SD = 0.06 [39, 40].

A further downscaling allows extension of the comparative study to the level of each of the 82 irrigation units. The average difference between SEBAL and SIWARE for the individual irrigation units was DE24/E24 = −0.08 (SD = 0.26). With the exception of units 15, 19, and 27, the results were encouraging (see Fig. 5). For all 82 irrigation units together, daily values of SEBAL were found to be 5.1% higher than the SIWARE predictions. A 5.1% deviation is within the allowable range of the SIWARE model accuracy (10% on an annual basis). Hence, the error in evaporation from remote sensing increases as one goes from extensive composite regions (5.1% deviation) via command areas (8% deviation ±6%) to isolated irrigation units (8% ± 26%) [39, 40].

4 ET MODIS Products

The MOD16 global ET/LE/ETc/potential LE datasets are consistent 1-km^2 ET databases. It covers the 109.03×10^6 km^2 global vegetated land areas, every 8-day, monthly, and annual periods from 2000 to 2014.

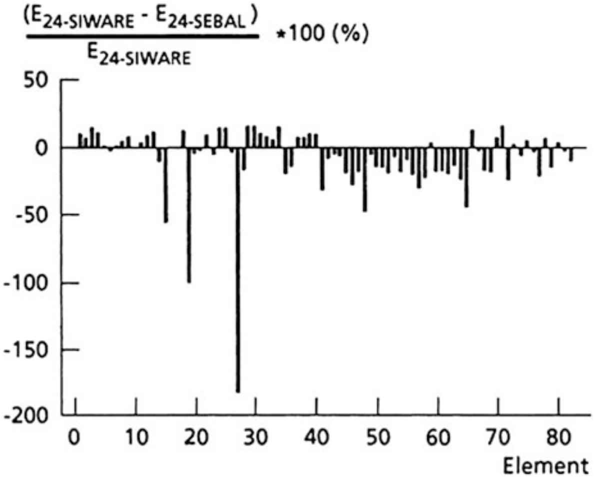

Fig. 5 Determination of the relative deviation DE/E for each of the 82 irrigation units of SIWARE on August 5, 1986. The average value turned out to be DE/E $= -0.08 \pm 0.26$ [39, 40]

The MOD16 ET datasets are estimated using Mu et al.'s developed ET algorithm [49] superior to the previous Mu et al.'s article [50]. The ET algorithm is calculated according to the Penman-Monteith equation [51]. Surface resistance is a sufficient resistance to transpiration from the plant canopy and evaporation from the land surface.

Physical ET involves evaporation from wet and moist soil, from rainwater prevented by the canopy before it touches the soil and the transpiration through stomata on crop leaves and stems. Evaporation of water appropriated by the canopy is a highly significant water flux for ecosystems with a high LAI. Canopy conductance for plant transpiration is estimated by applying LAI to scale stomatal conductance up to canopy level.

For several plant varieties during growing periods, stomatal conductance is regulated by VPD [50] and daily minimum air temperature (T_{min}). T_{min} is used to control latent and dynamic growing seasons for evergreen biomes. High temperatures are often followed by high VPDs, directing to the incomplete or full closing of stomata.

4.1 A Case Study for ET MODIS Calibration Under Egyptian Conditions

A case study on Nile Delta was investigated by El-Shirbeny et al. [52]. The flowchart of the used methodology is shown in Fig. 6. The MODIS16 ET data were validated under Egyptian conditions. The changing in weather condition and/or changing in vegetation cover means changing in ETa. The mean of ETa according to MODIS

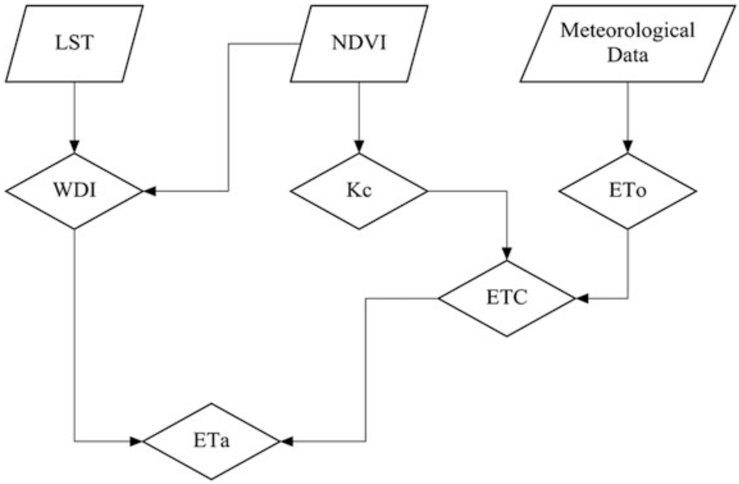

Fig. 6 Explains the method of ET MODIS's calibration

product was changed, and the results were 45.6, 50.2, and 45.4 (mm/month) at years 2002, 2007, and 2013, respectively. On the other hand, the mean of ETa according to estimated method changed, and the results were 56.6, 62.7, and 57.4 (mm/month) at years 2002, 2007, and 2013, respectively (Fig. 7). The northern part of the study area consumes water more than the southern part because of rice cultivation in summer in this part which consumes a lot of water; on the other hand, rice cultivation is not allowed in the southern part. In the last decade, the government started developing field irrigation systems in the northern part of Nile Delta shared with the German government.

From Figs. 8 and 9, there are two seasons; the first one starts from the beginning of June and finishes at the end of September and the second from the beginning of November to the end of April. On the other hand, May and October almost are in-between seasons. The maximum ETa according to MODIS product in 2002 and 2007 were 70.7 and 84.2 (mm/month) in August, respectively, but the minimum were 25.8 and 27 (mm/month) in October and June, respectively. In 2013, the minimum of ETa was 23 (mm/month) in May, and the maximum was 76.1 (mm/month) in July.

On the other hand, the maximum ETa according to WDI in 2002 and 2007 were 90.5 and 98.8 (mm/month) in August, respectively, but the minimum were 34.1 and 41.3 (mm/month) in May and November, respectively. In 2013, the minimum of ETa was 35.4 (mm/month) in May, and the maximum was 94.8 (mm/month) in July. Linear relation between ETa based on MODIS product and ETa based on estimated method was established with R2 as high as 0.86 (Fig. 10).

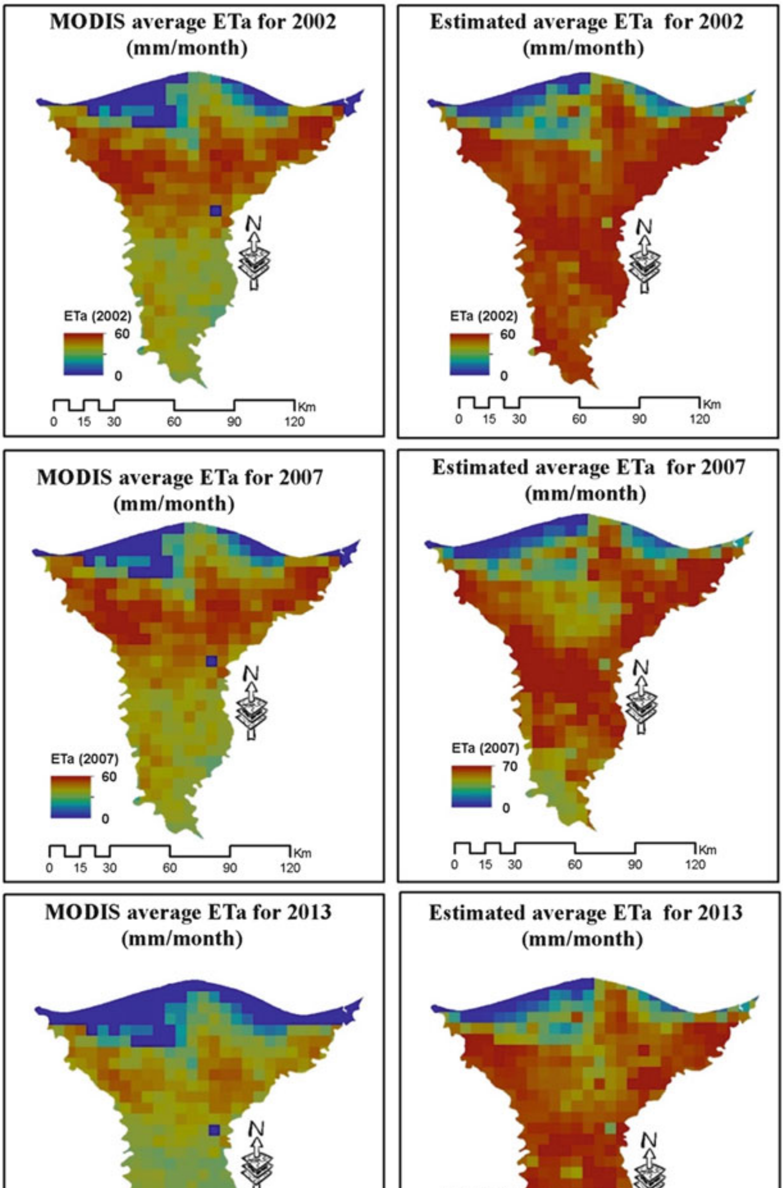

Fig. 7 Annual average ETa maps according to MODIS product and estimated method at years 2002, 2007, and 2013 [52]

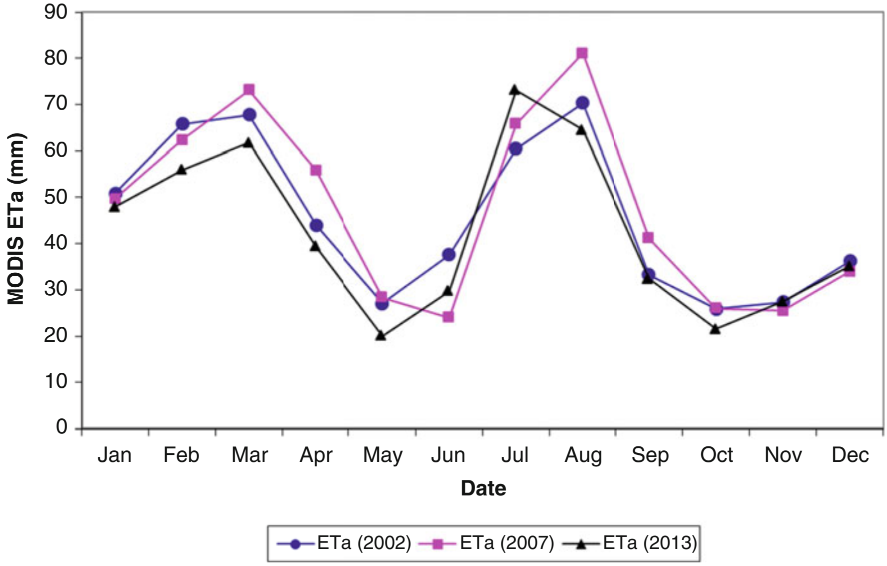

Fig. 8 Monthly MODIS ETa product (mm/month) at years of 2002, 2007, and 2013 [52]

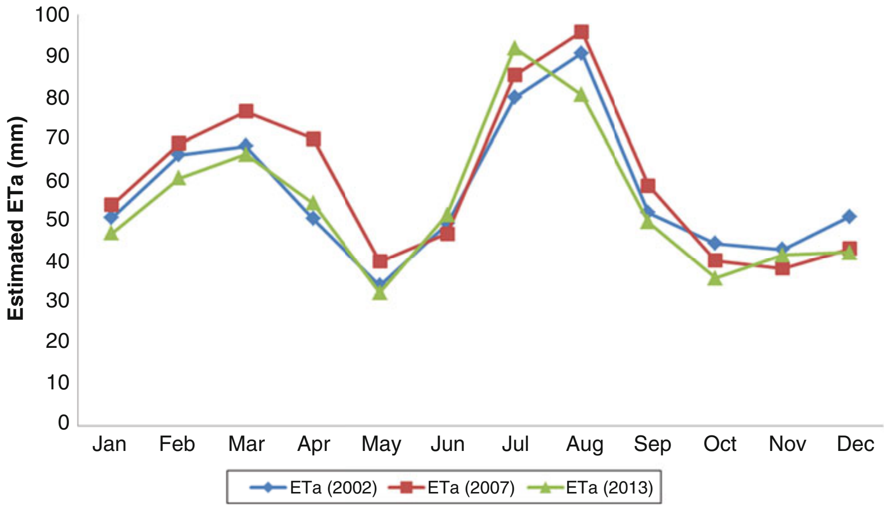

Fig. 9 Monthly estimated ETa (mm/month) at years of 2002, 2007, and 2013 [52]

5 Conclusion

Crop water consumption has to be estimated with a high level of accuracy to save water and to maximize water unit uses. The limitation of water resources and scarcity of water in arid and semiarid regions put many countries in critical situation. Dealing

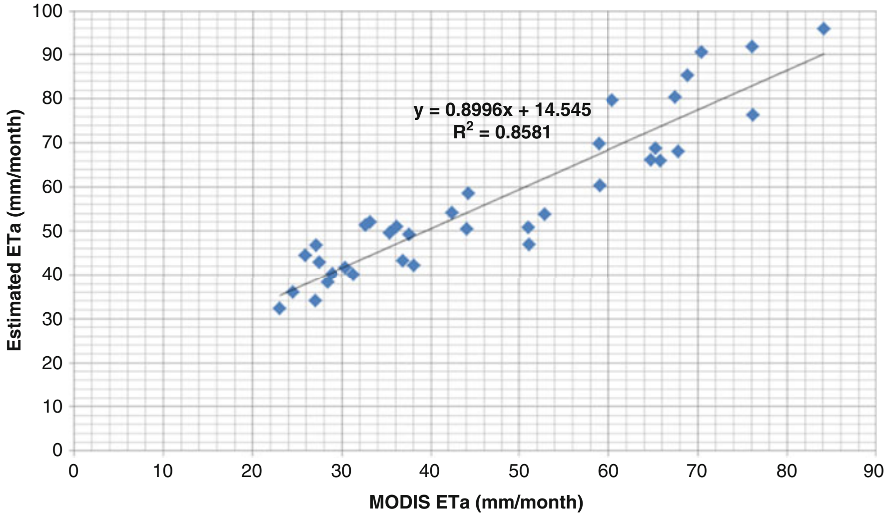

Fig. 10 The relation between MODIS ETa product and estimated ETa [52]

with water shortage must be planned, and good models were needed to estimate water consumption. Space-borne technologies are a good and powerful tool but need calibration and validation. Maybe in the future, it may be a stand-alone technology, but first, we must deal with it using new methods. It must have its own methodologies.

6 Recommendations

Remote sensing techniques are powerful on the large scale if it is used after calibration and validation. Developing the old methods of calculation, the irrigation water consumption is necessary for estimation accuracy. Numerous ET calculation models are so complicated and it needs to be the simplest.

References

1. Buffum BC (1892) Irrigation and duty of water. Wyo Agric Exp Bull 8
2. Allen RG, Pereira LS, Raes D, Smith M (1998) Crop evapotranspiration: guidelines for computing crop water requirements. United Nations Food and Agriculture Organization, irrigation and drainage paper no. 56. FAO, Rome
3. Lebon E, Dumas V, Pieri P, Schultz HR (2003) Modelling the seasonal dynamics of the soil water balance of vineyards. Funct Plant Biol 30(6):699–710

4. El-Shirbeny MA, Aboelghar MA, Arafat SM, El-Gindy AGM (2014) Assessment of the mutual impact between climate and vegetation cover using NOAA-AVHRR and Landsat data in Egypt. Arab J Geosci 7(4):1287–1296
5. El-Shirbeny MA, Saleh NH, Ali AM (2014) Estimation of potential crop evapotranspiration using remote sensing techniques. In: Proceedings of the 10th international conference of AARSE, pp 460–468
6. Hu G, Jia L, Menenti M (2015) Comparison of MOD16 and LSA-SAF MSG evapotranspiration products over Europe for 2011. Remote Sens Environ 156:510–526
7. Merlin O, Chirouze J, Olioso A, Jarlan L, Chehbouni G, Boulet G (2014) An image-based four-source surface energy balance model to estimate crop evapotranspiration from solar reflectance/thermal emission data (SEB-4S). Agric For Meteorol 184:188–203
8. Rwasoka DT, Gumindoga W, Gwenzi J (2011) Estimation of actual evapotranspiration using the Surface Energy Balance System (SEBS) algorithm in the Upper Manyame catchment in Zimbabwe. Phys Chem Earth 36:736–746
9. Tadesse T, Senay GB, Berhan G, Regassa T, Beyen S (2015) Evaluating a satellite-based seasonal evapotranspiration product and identifying its relationship with other satellite-derived products and crop yield: a case study for Ethiopia. Int J Appl Earth Obs Geoinf 40:39–54
10. Wojtowicz M, Wojtowicz A, Piekarczyk J (2016) Application of remote sensing methods in agriculture. Commun Biometry Crop Sci 11:31–50
11. Oki T, Kanae S (2006) Global hydrological cycles and world water resources. Science 313:1068–1072
12. French AN, Hunsaker DJ, Thorp KR (2015) Remote sensing of evapotranspiration over cotton using the TSEB and METRIC energy balance models. Remote Sens Environ 158:281–294
13. Ghulam A, Li Z, Qin Q, Yimit h, Wang J (2008) Estimating crop water stress with ETM+ NIR and SWIR data. Agric For Meteorol 148:1679–1695
14. Tasumi M, Allen RG (2007) Satellite-based ET mapping to assess variation in ET with timing of crop development. Agric Water Manag 88:54–62
15. Choudhury BJ (1997) Global pattern of potential evaporation calculated from the Penman Monteith equation using satellite and assimilated data. Remote Sens Environ 61(1):64–81
16. Moran MS, Clarke TR, Inoue Y, Vidal A (1994) Estimating crop water deficit using the relation between surface air temperature and spectral vegetation index. Remote Sens Environ 49:246–263
17. Bastiaanssen WGM, Roest CWJ, Pelgrum H, Abdel Khalek MA (1992) Monitoring of the irrigation performance on the basis on actual evapotranspiration: comparison of satellite data and simulation model results. In: Feyen J, Mwendera E, Badji M (eds) Advances in planning, design and management of irrigation systems as related to sustainable land use. Center for Irrigation Engineering and ECOWARM, Leuven, pp 473–483
18. Dibella CM, Rebella CM, paruelo JM (2000) Evapotranspiration estimates using NOAA AVHRR imagery in the Pampa region of Argentina. Int J Remote Sens 21(4):791–797
19. Ray SS, Dadhwal VK (2001) Estimation of evapotranspiration of irrigation command area using remote sensing and GIS. Agric Water Manag 49:239–249
20. Kerdiles H, Groundena M, Rodrignes R, Seguin B (1996) Forest mapping using NOAA-AVHRR data in the Pampean region, Argentina. Agric For Meteorol 79:157–182
21. Kalma JD, Mcvicar TR, Mccabe MF (2008) Estimating land surface evaporation: a review of methods using remotely sensed surface temperature data. Surv Geophys 29:421–469
22. Alderfasi AA, Nielsen DC (2001) Use of crop water stress index for monitoring water status and scheduling irrigation in wheat. Agric Water Manag 47(1):69–75
23. Li L, Nielsen DC, Yu Q, Ma L, Ahuja LR (2010) Evaluating the crop water stress index and its correlation with latent heat and CO_2 fluxes over winter wheat and maize in the North China plain. Agric Water Manag 97(8):1146–1155
24. Méndez-Barroso LA, Garatuza-Payán J, Vivoni ER (2008) Quantifying water stress on wheat using remote sensing in the Yaqui Valley, Sonora, Mexico. Agric Water Manag 95(6):725–736

25. Yuan G, Luo Y, Sun X, Tang D (2004) Evaluation of a crop water stress index for detecting water stress in winter wheat in the North China Plain. Agric Water Manag 64:29–40
26. Jackson RD, Idso SB, Reginato RJ, Pinter JR (1981) Canopy temperature as a crop water stress indicator. Water Resour 17:1133–1138
27. Choudhury BJ (1983) Simulating the effects of weather variables and soil water potential on a corn crop canopy temperature. Agric Meteorol 29:169–182
28. Hiler EA, Clark RN (1971) Stress day index to characterize effects of water stress on crop yields. Transa Hydrol (210-VI-NEH)
29. Erdem Y, Sehirali S, Erdem T, Kenar D (2006) Determination of crop water stress index for irrigation scheduling of bean (Phaseolus vulgaris L.). Turk J Agric For 30:195–202
30. Garcia M, Fernández N, Villagarcía L, Domingo F, Puigdefábregas J, Sandholt I (2014) Accuracy of the temperature–vegetation dryness index using MODIS under water-limited vs. energy-limited evapotranspiration conditions. Remote Sens Environ 149:100–117
31. Clarke TR (1997) An empirical approach for detecting crop water stress using multi-spectral airborne sensors. Horticult Technol 7:9–16
32. El-Shirbeny MA, Ali AM, Mohamed ES, Abutaleb K, Bauomy EM (2017) Monitoring of actual evapotranspiration using remotely sensed data under modern irrigation systems. J Geograph Environ Earth Sci Int 12(4):1–12
33. Rana G, Katerji N (2000) Measurement and estimation of actual evapotranspiration in the field under Mediterranean climate: a review. Eur J Agron 13:125–153
34. Er-Raki S, Chehbouni A, Guemouria N, Duchemin B, Ezzahar J, Hadria R (2007) Combining FAO-56 model and ground-based remote sensing to estimate water consumption of wheat crops in semi-arid regions. Agric Water Manag 87:41–54
35. Dardanelli JL, Ritchie JT, Calmon M, Andrianiand JM, Collino DJ (2004) An empirical model for root water uptake. Field Crop Res 87:59–71
36. Kustas WP, Norman JM (1999) Evaluation of soil and vegetation heat flux predictions using a simple twosource model with radiometric temperatures for partial canopy cover. Agric For Meteorol 94:13–29
37. Kiehl JT, Trenberth KE (1997) Earth's annual global mean energy budget. Bull Am Meteorol Soc 78:197–208
38. Su Z (2002) The Surface Energy Balance System (SEBS) for estimation of turbulent heat fluxes. Hydrol Earth Syst Sci 6(1):85–99
39. Bastiaanssen WGM, Menenti M, Feddes RA, Holtslag AAM (1998) A remote sensing surface energy balance algorithm for land (SEBAL) 1. Formulation. J Hydrol 212–213:198–212
40. Bastiaanssen WGM, Pelgrum J, Wang YM, Moreno JF, Roerink GJ, van der Wal T (1998) A remote sensing surface energy balance algorithm for land (SEBAL) Part 2: validation. J Hydrol 212–213:213–229
41. Bastiaanssen WGM (2000) SEBAL-based sensible and latent heat fluxes in the irrigated Gediz Basin, Turkey. J Hydrol (Amst) 229:87–100
42. Allen RG, Tasumi M, Trezza R (2007) Satellite-based energy balance for mapping evapotranspiration with internalized calibration (METRIC) model. J Irrig Drain Eng 133(4):380–393
43. Wu BF, Xiong J, Yan N (2008) ETWatch for monitor regional evapotranspiration with remote sensing. Adv Water Sci 19(5):671–678
44. Wu BF, Xiong J, Yan N (2011) ETWatch: models and methods. J Remote Sens 15(2):224–230
45. Menenti M, Choudhury B (1993) Parameterization of land surface evaporation by means of location dependent potential evaporation and surface temperature range. In: Bolle HJ, Feddes RA, Kalma JD (eds) Exchange processes at the land surface for a range of space and time scales, vol 212. IAHS, Oxfordshire, pp 561–568
46. Verhoef W (1996) Application of harmonic analysis of NDVI time series (HANTS). In: Azzali S, Menenti M (eds) Fourier analysis of temporal NDVI in the Southern African and American continents. DLO Win and Staring Centre, Report, 108, Wageningen, pp 19–24
47. Pelgrum H (1992) Mapping areal surface energy balances during daytime using Meteosat data. Internal note 195. DLO Winand Staring Centre, Wageningen, p 50

48. Abdel-Gawad ST, Abdel Khalek MA, Boels D, El-Quosy DE, Roest CWJ, Rijtema PE, Smit MFR (1991) Analysis of water management in the Eastern Nile Delta. Reuse Report 30. DLO Winand Staring Center, Wageningen, p 245
49. Mu Q, Zhao M, Running SW (2011) Improvements to a MODIS global terrestrial evapotranspiration algorithm. Remote Sens Environ 115(8):1781–1800
50. Mu Q, Heinsch FA, Zhao M, Running SW (2007) Development of a global evapotranspiration algorithm based on MODIS and global meteorology data. Remote Sens Environ 111:519–536
51. Monteith JL (1965) Evaporation and environment. In: Fogg BD (ed) The state and movement of water in living organism, symposium of the society of experimental biology, vol 19. Cambridge University Press, Cambridge, pp 205–234
52. El-Shirbeny MA, Alsersy MAM, Saleh NH, Abu-Taleb KA (2015) Changes in irrigation water consumption in the Nile Delta of Egypt assessed by remote sensing. Arab J Geosci 8:10509–10519